J Mater Sci (2008) 43:6925–6932
DOI 10.1007/s10853-008-2988-0

Synthesis and microstructure of vertically aligned ZnO nanowires grown by high-pressure-assisted pulsed-laser deposition

L. C. Tien · S. J. Pearton · D. P. Norton ·
F. Ren

Received: 26 February 2008 / Accepted: 2 September 2008 / Published online: 27 September 2008

Abstract The microstructure and growth behavior for vertically aligned Zinc oxide (ZnO) nanowires, synthesized on a ZnO thin film template by pulsed-laser deposition (PLD), is reported. The nanowire growth proceeds without any metal catalyst for nucleation, although an epitaxial ZnO thin film template is necessary in order to achieve uniform alignment. Nanowire growth at argon or oxygen background pressures of 500-mTorr results in nanowire diameters as small as 50–90 nm, with diameters largely determined by growth pressure and temperature. Room temperature photoluminescence show both near-band-edge and deep-level emission. The deep-level emission is believed caused by oxygen vancancies formed during growth.

Introduction

The synthesis of one-dimensional (1D) semiconductor nanostructures has attracted great interest due to the unique physical and chemical properties of these materials. Zinc oxide (ZnO) [1] is a wide-band-gap n-type semiconductor with direct band gap of 3.37 eV that has been extensively studied due to its applicability in transparent electronics [2–4], chemical and gas sensors [5–11], spin functional devices [12–16], Schottky diodes [17, 18], nanoelectronics [19], and blue light-emitting diodes [20–23]. The synthesis of ZnO nanowires [24] has been reported using a variety of methods, including thermal evaporation [25], molecular beam epitaxy [26], solution-phase growth [27], hydrothermal methods [28, 29], and pulsed-laser deposition (PLD) [30–32]. Vertically aligned ZnO nanowires are potentially useful for vertical device fabrication, with proposed device implementations that include light-emitting-diodes [23, 33], dye-sensitized solar cells [27, 34], and nanopiezoelectrics [35]. Considerable effort has been made to fabricate aligned ZnO nanowires on various substrates using either physical vapor deposition (PVD) [36], chemical vapor deposition (CVD) [37, 38], or metal-organic chemical vapor deposition (MOCVD) [39, 40]. It remains challenging to controllably grow well-aligned ZnO nanowires. In many cases, the growth of semiconductor nanowires proceeds via a vapor–liquid–solid (VLS) growth mechanism that requires a metals catalyst. However, metal catalysts can also serve as impurities in the nanowires, thus limiting material properties.

In this article, the growth of vertically aligned ZnO nanowires by high-pressure-assisted PLD is reported. This technique for nanowire growth [30–32] requires a ZnO template for nucleation, but proceeds without the use of any metal catalyst. The structure and properties of the nanowires are characterized, revealing high-quality single crystal ZnO nanowires. The effects of growth temperature and background pressure on nanowire growth and properties are discussed. While previous work focused on growth at pressures greater than 1 Torr resulting in ZnO nanowire diameters of 120 nm or more, the present experiments

---

L. C. Tien
Department of Materials Science and Engineering,
National Dong Hwa University, Shoufeng, Hualien 974, Taiwan
e-mail: lctien@mail.ndhu.edu.tw

S. J. Pearton · D. P. Norton (✉)
Department of Materials Science and Engineering,
University of Florida, Gainesville, FL 32611, USA
e-mail: dnort@mse.ufl.edu

F. Ren
Department of Chemical Engineering, University of Florida,
Gainesville, FL 32611, USA

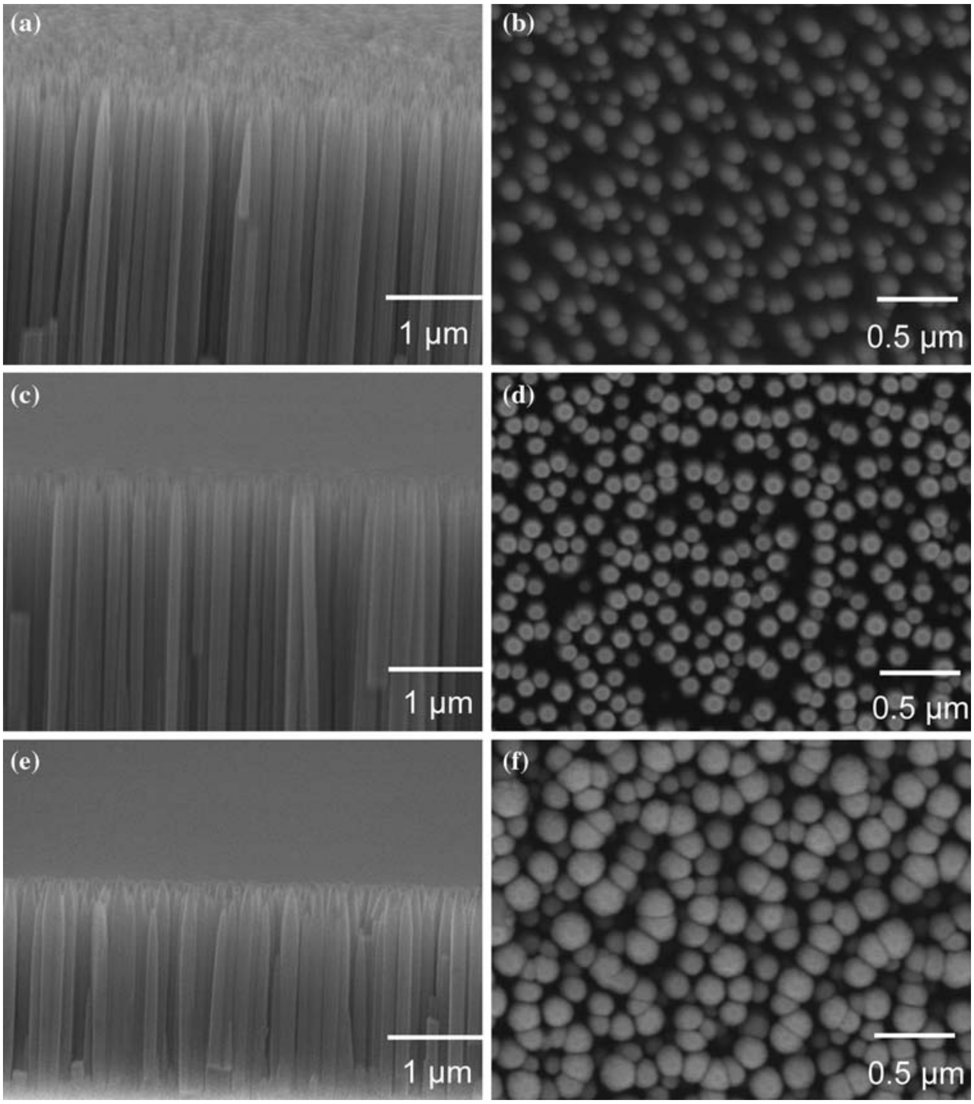

Fig. 1 FE-SEM images of well-aligned ZnO nanowires grown on a ZnO thin film template in (**a**, **b**) 500-mTorr pure oxygen, (**c**, **d**) 500-mTorr pure argon, and (**e**, **f**) a 325 mTorr/175-mTorr argon/oxygen mixture

examine lower deposition pressure, realizing significantly smaller nanowire diameters. Since PLD is a convenient means for achieving stoichiometric transfer in growing multi-element materials [41], these results suggest the possibility of growing oxide nanowires with complex crystal structures and/or multi-cation stoichiometry.

Experimental section

Pulsed-laser deposition was used for the ZnO nanowire growth. The ablation target was fabricated using high-purity ZnO (99.9995%). The target was pressed and sintered at 1,000 °C for 12 h in air. A KrF excimer laser was used as the ablation source. A repetition rate of 5 Hz was used, with target to substrate distance of 2.5 cm and a laser pulse energy density of 1–3 J/cm^2. The growth chamber exhibits

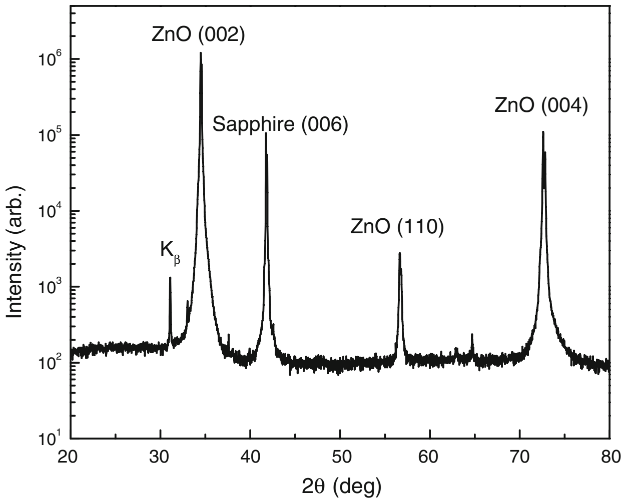

Fig. 2 XRD θ-2θ scan of ZnO nanowires grown at 800 °C in 500-mTorr Ar

a base pressure of 10^{-6} Torr. In order to achieve well-ordered ZnO nanowires, a thin (75–200 nm) ZnO template layer was grown on the c-plane sapphire substrate prior to nanowire nucleation. The ZnO template layer was grown at 450 °C in 30 mTorr of oxygen. The repetition rate of the laser was 5 Hz. Deposition time was 20 min, resulting in a c-axis oriented ZnO template layer thickness of approximately 200 nm. Prior to deposition, the substrates were ultrasonically cleaned with trichloroethylene, acetone, and methanol, followed by compressed N_2 drying. The substrates were attached to the heater using Ag paint. Prior to growth, the target was cleaned in situ by pre-ablating with approximately 2,000 shots. The growth experiments were performed over a temperature range of 500–800 °C in a background pressure of 150–500 mTorr. Three different gas ambient (O_2, Ar, and O_2/Ar mixture) were used to investigate the effects of oxidation and gas-phase collisions in the formation of nanowires. The typical growth time was 2 h. After growth, the samples were cooled under the same gas ambient as was used during growth. The as-grown samples were characterized using X-ray diffraction (XRD) (Philips 3720, Cu-Kα), field emission scanning electron microscopy (FE-SEM) (JEOL 6335F), and high-resolution transmission electron microscopy (HRTEM) (JEOL 2010F). The optical properties of the nanowires were examined using photoluminescence at room temperature. A He–Cd (325 nm) laser was used as the excitation source.

Results and discussion

In general, nanowire growth was achieved via PLD growth at relatively high temperature and high background pressure. Figure 1 shows cross-section and plan-view SEM images of ZnO nanowire arrays grown at 800 °C in 500-mTorr oxygen, 500-mTorr argon, or a 325-mTorr Ar/175-mTorr O_2 mixture. In the case of pure argon, the only oxygen supplied during growth was from the ZnO in the ablation plume. Vertically aligned nanowires were observed by cross-sectional FE-SEM. HRTEM of individual nanowires shows that the growth is highly c-axis oriented along the normal direction of the substrate. At low

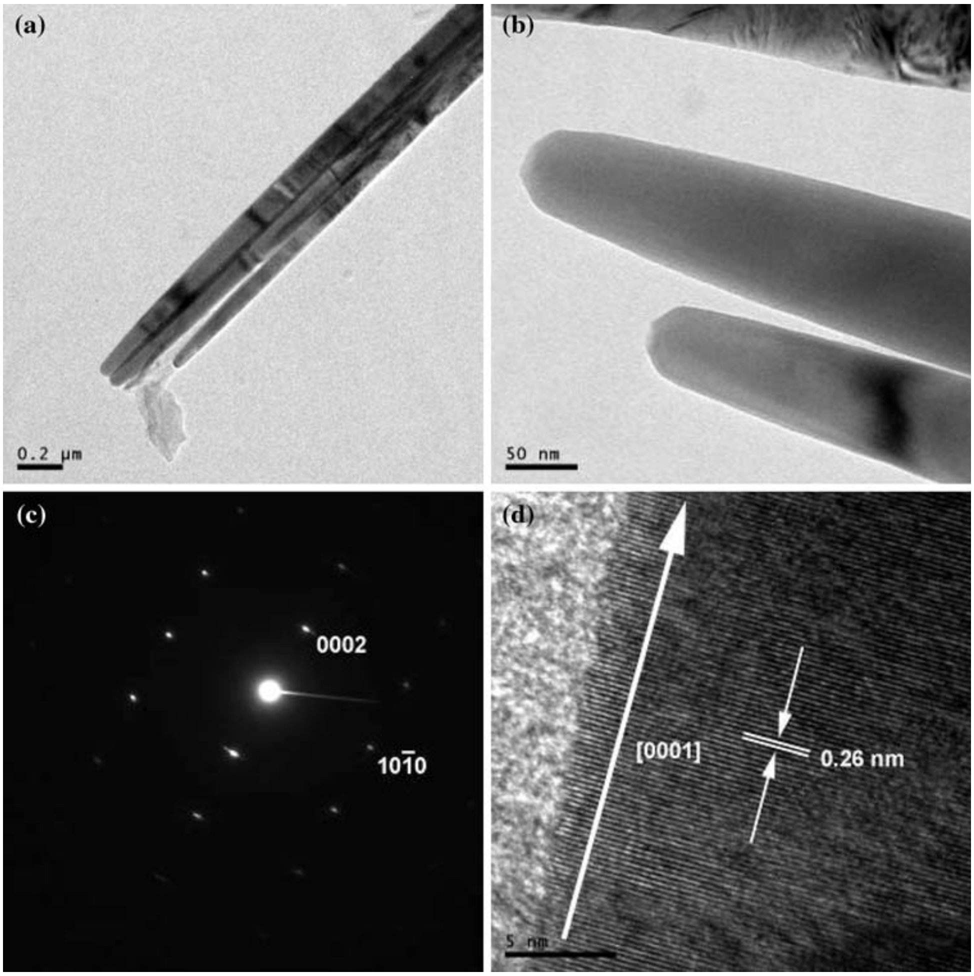

Fig. 3 Low magnification (**a**, **b**) TEM images of ZnO nanowires grown on a ZnO thin film at 800 °C in 500-mTorr Ar. Also shown is (**c**) a selected-area electron diffraction pattern taken from a single ZnO nanowire, showing the single crystal wurtzite structure, as well as (**d**) an HRTEM image of a single ZnO nanowire showing lattice fringes

magnification, a relatively uniform distribution of diameter is observed for the nanowires. The diameters are around 50–90 nm. Moreover, the nanowires grow as a high-density array and are distributed over the entire substrate. For the samples in Fig. 1, the length of the nanowires was approximately 6 μm. At high magnification, nanowires with smooth hexagonal facets can be observed. As expected, no catalyst particles are observed on the tips of the nanowires, which indicates that the nanowire growth does not proceed by a VLS mechanism. The composition of the nanowires was investigated by Energy-dispersive X-ray (EDX) analysis. The results indicate that the nanowires are composed of zinc and oxygen with no significant impurities found in the EDX data.

The orientation and crystalline properties of the ZnO nanowires was characterized with XRD and transmission electron microscopy (TEM). Figure 2 shows the XRD patterns for the ZnO nanowires shown in Fig. 1 grown in pure argon. Two sharp ZnO (002) and (004) peaks with high intensity dominate the diffraction patterns, consistent with ZnO nanowires that are principally oriented along the c-axis. A relatively weak ZnO (110) peak is also observed. Note that the XRD intensity is plotted on a log scale. Nevertheless, the ZnO (110) peak indicates that some fraction of the deposited material is not c-axis oriented. The patterns can be indexed to the ZnO hexagonal wurtzite structure with lattice constants of $a = 0.325$ nm and $c = 0.512$ nm. Additional structure characterization was carried out using TEM. Figure 3a shows low-magnification images for parallel nanowires that were mechanically removed from the substrate. The nanowires have a relatively uniform diameter (50–90 nm) and are a few micrometers in length. Note that no secondary phase particles are observed at the top or bottom of the nanowires. These results are consistent with the FE-SEM observations as shown in Fig. 1. The images in Fig. 3b show that the

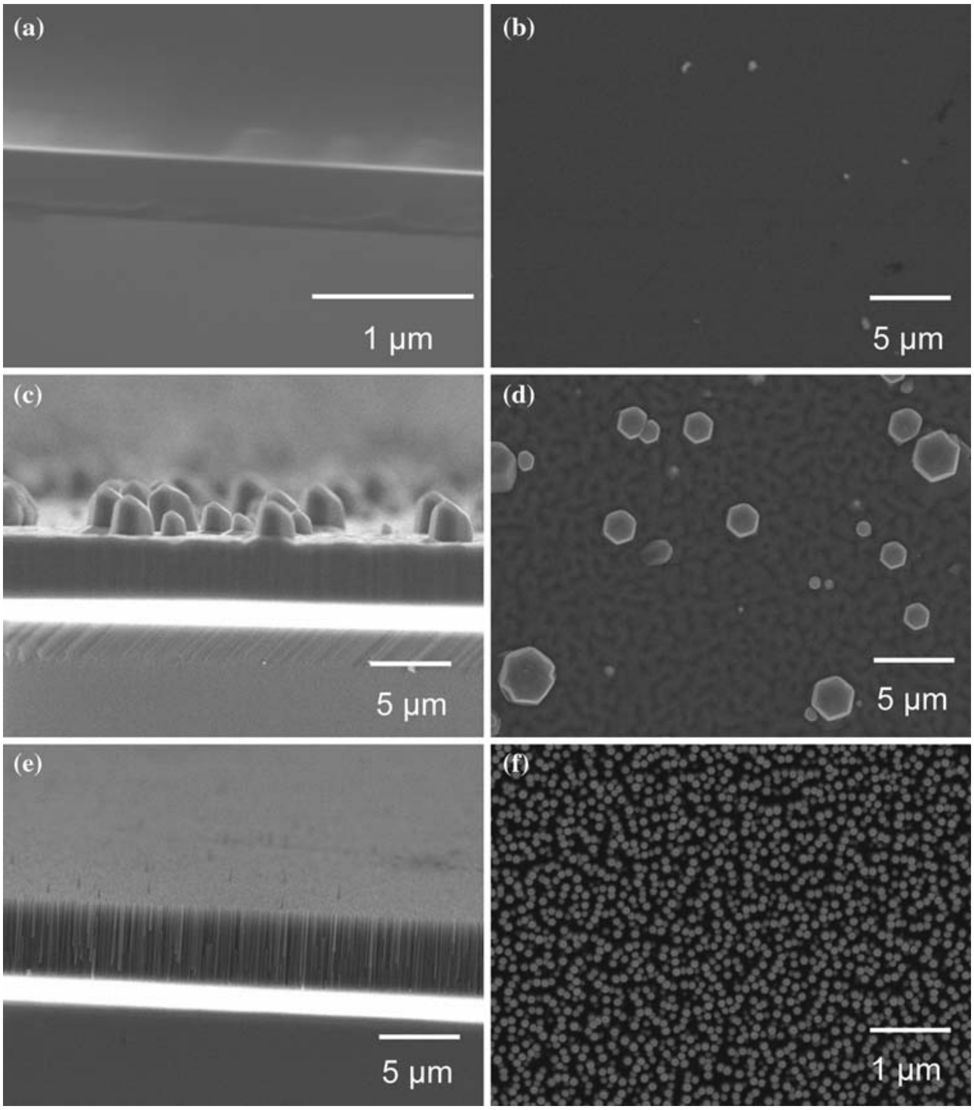

Fig. 4 Cross-sectional and top view FE-SEM images of the ZnO nanowires grown at 800 °C in pure oxygen with oxygen background pressures of (**a**, **b**) 150 mTorr, (**c**, **d**) 300 mTorr, and (**e**, **f**) 500 mTorr

nanowires are tapered and faceted at the ends. In order to further investigate the structure, selected-area electron diffraction was performed on a single nanowire. The pattern is consistent with a single crystal wurtzite structure. Figure 3d shows the HRTEM images, showing that the nanowire is structurally uniform and no discernable defects. In the high-resolution images, lattice fringes show lattice spacing of 0.26 nm, which corresponds to 1/2 of the c-axis lattice constant, confirming that the ZnO nanowires are oriented in the c-axis direction. Since the (001) planes of ZnO are the closest packed plane, stacking along the c-axis is the most energetically favorable. This growth direction is commonly observed in ZnO nanowires.

The morphology and microstructure of the nanowires were examined as a function of growth conditions, in particular total background pressure, oxygen pressure, and substrate temperature. Figure 4 shows the FE-SEM images of samples deposited in pure oxygen at O_2 pressures ranging from 150 to 500 mTorr. The growth temperature was 800 °C. All samples were grown on a thin template layer of ZnO on the sapphire substrate. At a growth pressure of 150-mTorr O_2, the deposited ZnO consists of a continuous, smooth thin film as seen in Fig. 4a and b. Increasing the oxygen pressure to 300 mTorr resulted in the nucleation and growth of oriented microcrystals with hexagonal facets as seen in Fig. 4c. The size of microcrystals varies from 1 to 5 μm, growing normal to the substrate. When the pressure was further increased to 500 mTorr, the growth mode undergoes a transition from continuous thin film to highly aligned nanowire growth. A highly dense array of nanowires with hexagonal facets is observed. The nanowires are oriented with their c-axis perpendicular to the surface with relatively uniform diameter and density. Note that very few nanowires were

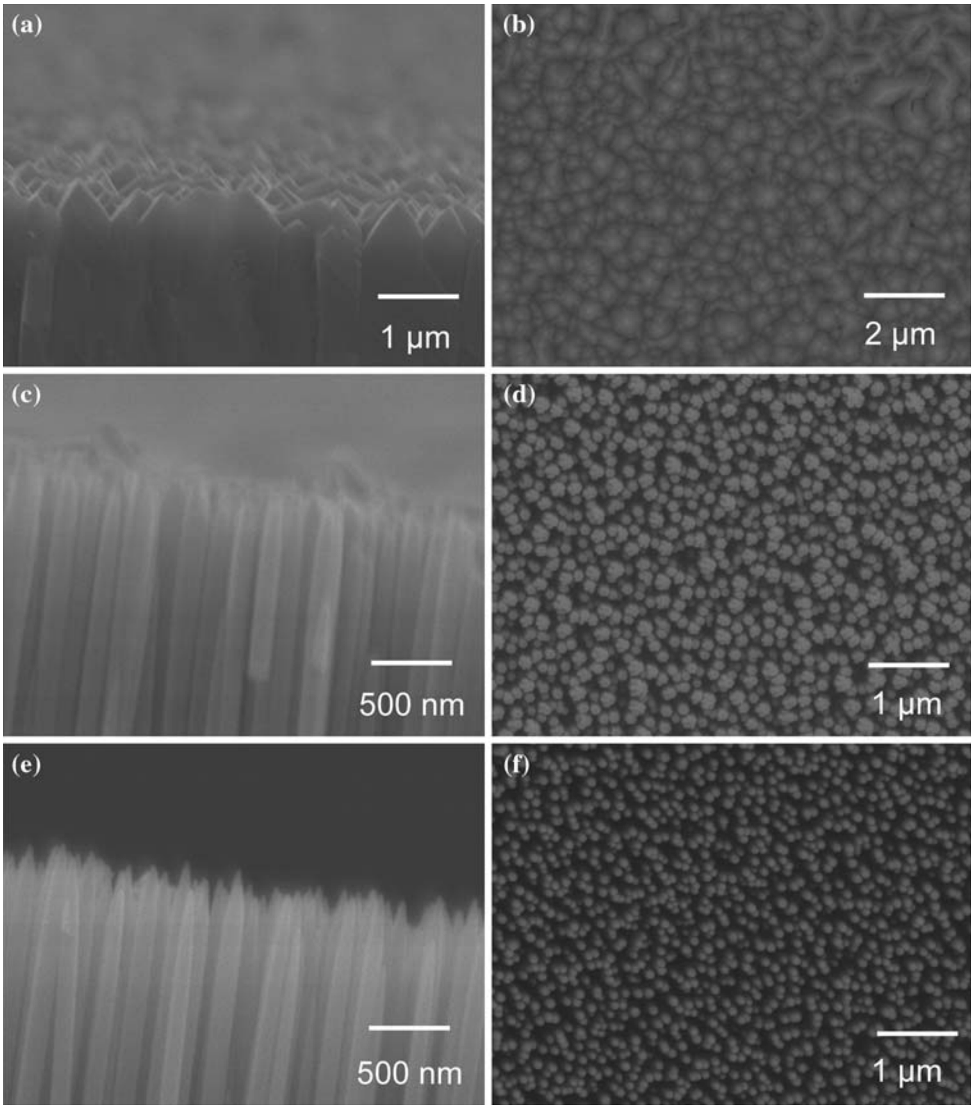

Fig. 5 Cross-sectional and top view FE-SEM images of the ZnO nanorods grown under 500 mTorr of oxygen at different temperatures. (**a**, **b**) 550 °C, (**c**, **d**) 750 °C, (**e**, **f**) 800 °C, respectively

obtained when the pressure was further increased to 1 Torr. For PLD at growth pressures of 200 mTorr or less, it is well known that kinetic energy of the ablated species enhances surface mobility of deposited species. At the higher pressures, the ablation plume is completely thermalized with no non-thermal component. This largely explains the dependence of nanowire formation on background pressure.

In addition to pressure, the effect of substrate temperature in the formation of nanowires was also examined. Figure 5 shows the cross-sectional and plan-view FE-SEM images of ZnO nanorods grown at an oxygen pressure of 500 mTorr at temperatures ranging from 550 to 800 °C. At 550 °C (Fig. 5a and b), the diameters of the nanowires are on the order of 500 nm. At 750 °C, the diameter is reduced to approximately 150 nm. At 800 °C, the diameter of the nanowires is less than 100 nm. One explanation for this temperature dependency of nanowire diameter relates to surface diffusion. A higher surface mobility is realized for higher growth temperatures. High temperatures provide sufficient energy for deposited species from the ablation target to migrate to low-energy sites for growth. If substrate temperature is low (<650 °C), surface species will remain at higher energy sites, thus yielding large diameter nanowires or simply rough, granular films. In order to achieve one-dimensional growth, it is important to provide sufficient surface mobility for species to reach low-energy nucleation sites.

The variation in optical properties for the ZnO nanowires grown in different background ambients was investigated using room temperature photolumienscence measurements. Figure 6a shows the typical room temperature PL spectra of the ZnO nanowires grown at 800 °C and 500-mTorr oxygen. A weak near-band-edge-emission in the UV region at 380 nm and a strong broad band deep-level-emission at 520 nm is observed. The green band around 520 nm is commonly attributed to deep-level or trap-state emission due to vacancies and/or interstitials of zinc and oxygen in the crystal [42, 43]. In order to further investigate the origin of deep-level emissions, PL measurements were carried out for nanowires grown using the three different ambients (500-mTorr O_2, 500-mTorr Ar and 175-mTorr O_2/325-mTorr Ar mixture) at 800 °C. The near-band-edge-emission was higher for nanowires grown using pure argon. However, the deep-level emission was enhanced as well, suggesting a high density of defects due to the oxygen deficient ambient. In order to investigate this further, nanowires grown using the argon/oxygen mixture were examined. The near-band-edge-emission intensity increased 20 times relative to nanowires grown using pure oxygen. However, the broad green emission remained unchanged in the spectra for all cases. A plot of PL spectra for nanowires grown in the different background gases is shown in Fig. 6b. The results show that the deep-level emission persists in all ambients considered. The large deep-level emission was also observed on high-temperature grown nanowires. Liu et al. attributed modification in ZnO nanowire PL properties to size effects and oxygen stochiometry [44].

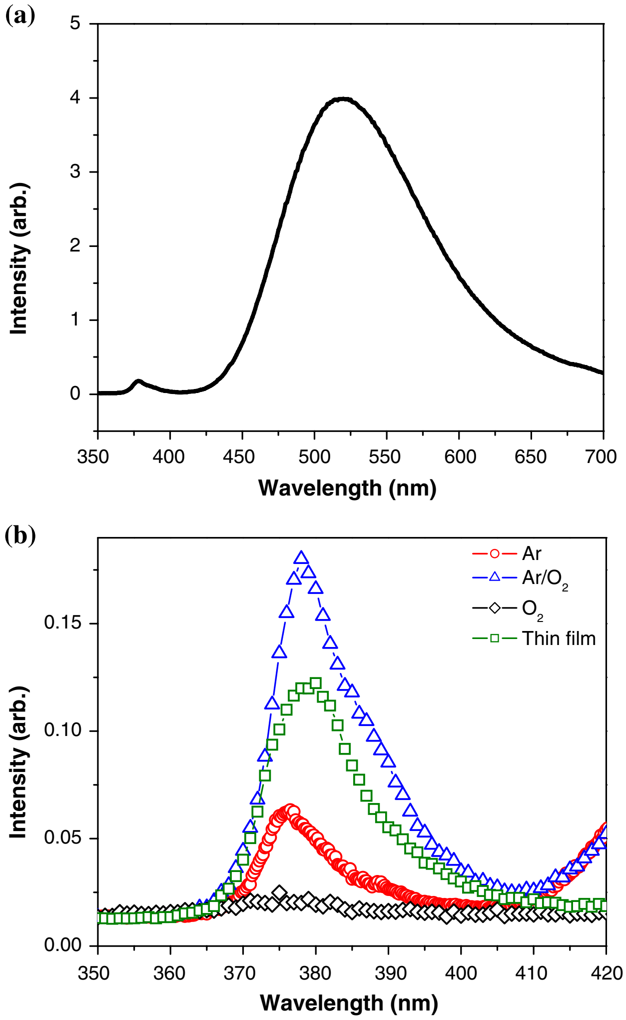

Fig. 6 (**a**) Room temperature PL spectra of ZnO nanowires grown at 800 °C in 500 mTorr (**b**) near-band-edge-emission of ZnO thin film and ZnO nanowires grown under different background ambient at 800 °C

In previous efforts to grow ZnO nanowires by PLD, the focus has been on a deposition pressure range of 1 Torr or greater [30–32]. At these pressures, the gas-phase collisions yield ZnO nanoparticle formation in the ablation plume. Based on this, the condensation of ablated particles in the laser ablation plume is assumed to play an important role in the nanorod growth. In the present study, the background pressures used are approaching the limit where the ablated nanoparticles can form. As such, it is unclear if the same growth mechanism holds for growth pressures of

500 mTorr as compared to 1–5 Torr. It should also be noted that the minimum diameter of the ZnO nanowires realized in this study (50 μm) are less than half seen for the nanowires reported at the high-deposition pressures. The trend towards smaller nanowire diameters at the lower background pressure is in agreement with the previous efforts. Future work will examine the transport properties of individual PLD-grown nanowires and compare their properties to those grown by other techniques [45–48]. One parameter that was not considered in this study but will have an impact on nanowire properties is growth rate as controlled by laser repetition rate. It has been shown in multiple studies on film growth using PLD that grain size varies in deposition rate. Future studies on nanowire growth should address this issue as well.

Conclusion

To summarize, vertically well-aligned ZnO nanowires with uniform diameters were fabricated on a ZnO thin film template by high-pressure-assisted PLD. The morphology and structure were characterized by FE-SEM, XRD, and HRTEM. No metal catalyst was used. The results suggest the possibility of growing complex metal oxide nanostructures, including tailored heterostructures, with PLD [49–51].

Acknowledgements This work was supported by NASA Kennedy Space Center Grant NAG 10–316. The authors would also like to acknowledge the assistance of the staff member in the Major Analytical Instrumentation Center (MAIC) at the University of Florida.

References

1. Pearton SJ, Norton DP, Ip K, Heo YW, Steiner T (2003) Superlattices Microstruct 34:3. doi:10.1016/S0749-6036(03)00093-4
2. Carcia PF, McLean RS, Reilly MH, Nunes G Jr (2003) Appl Phys Lett 82:1117. doi:10.1063/1.1553997
3. Masuda S, Kitamura K, Okumura Y, Miyatake S, Tabata H, Kawai T (2003) J Appl Phys 93:1624. doi:10.1063/1.1534627
4. Heo YW, Kwon YW, Li Y, Pearton SJ, Norton DP (2005) J Electron Mater 34:409. doi:10.1007/s11664-005-0120-7
5. Fan Z, Wang D, Chang P-C, Tseng W-Y, Lu JG (2004) Appl Phys Lett 85:5923. doi:10.1063/1.1836870
6. Wan Q, Li QH, Chen YJ, Wang TH, He XL, Li JP et al (2004) Appl Phys Lett 84:3654. doi:10.1063/1.1738932
7. Li QH, Liang YX, Wan Q, Wang TH (2004) Appl Phys Lett 85:6389. doi:10.1063/1.1840116
8. Wang HT, Kang BS, Ren F, Tien LC, Sadik PW, Norton DP et al (2005) Appl Phys Lett 86:243503. doi:10.1063/1.1949707
9. Tien LC, Sadik PW, Norton DP, Voss LF, Pearton SJ, Wang HT et al (2005) Appl Phys Lett 87:222106. doi:10.1063/1.2136070
10. Kang BS, Heo YW, Tien LC, Norton DP, Ren F, Gila BP et al (2005) Appl Phys A 80:1029. doi:10.1007/s00339-004-3098-8
11. Wang HT, Kang BS, Ren F, Tien LC, Sadik PW, Norton DP et al (2005) Appl Phys A 81:1117. doi:10.1007/s00339-005-3310-5
12. Liu LQ, Xiang B, Zhang XZ, Zhang Y, Yu DP (2006) Appl Phys Lett 88:063104. doi:10.1063/1.2168510
13. Ronning C, Gao PX, Ding Y, Wang ZL, Schwen D (2004) Appl Phys Lett 84:783. doi:10.1063/1.1645319
14. Fukumura T, Jin Z, Kawasaki M, Shono T, Hasegawa T, Koshihara S et al (2001) Appl Phys Lett 78:958. doi:10.1063/1.1348323
15. Cui J, Zeng Q, Gibson UJ (2006) J Appl Phys 99:8
16. Pearton SJ, Norton DP, Heo YW, Tien LC, Ivill MP, Li Y et al (2006) J Electron Mater 35:862. doi:10.1007/BF02692541
17. Heo YW, Tien LC, Norton DP, Pearton SJ, Kang BS, Ren F et al (2004) Appl Phys Lett 85:2107. doi:10.1063/1.1791733
18. Polyakov AY, Smirnov NB, Kozhukhova EA, Vdovin VI, Ip K, Heo YW et al (2003) Appl Phys Lett 83:575. doi:10.1063/1.1594830
19. Heo YW, Tien LC, Kwon Y, Norton DP, Pearton SJ, Kang BS et al (2004) Appl Phys Lett 85:2274. doi:10.1063/1.1794351
20. Lim J-H, Kong C-K, Kim K-K, Park I-K, Hwang D-K, Park S-J (2006) Adv Math 18:2720. doi:10.1002/adma.200502633
21. Wei ZP, Lu YM, Shen DZ, Zhang ZZ, Yao B, Li BH et al (2007) Appl Phys Lett 90:042113. doi:10.1063/1.2435699
22. Jiao SJ, Zhang ZZ, Lu YM, Shen DZ, Yao B, Zhang JY et al (2006) Appl Phys Lett 88:031911. doi:10.1063/1.2166686
23. Jeong M-C, Oh B-Y, Ham M-H, Myoung J-M (2006) Appl Phys Lett 88:202105. doi:10.1063/1.2204655
24. Heo YW, Norton DP, Tien LC, Kwon Y, Kang BS, Ren F et al (2004) Mater Sci Eng Rep 47:1. doi:10.1016/j.mser.2004.09.001
25. Huang MH, Wu Y, Feick H, Tran N, Weber E, Yang P (2001) Adv Math 13:113. doi:10.1002/1521-4095(200101)13:2<113::AID-ADMA113>3.0.CO;2-H
26. Heo YW, Varadarajan V, Kaufman M, Kim K, Norton DP, Fleming PH (2002) Appl Phys Lett 81:3046. doi:10.1063/1.1512829
27. Greene LE, Law M, Tan DH, Montano M, Goldberger J, Somorjai G et al (2005) Nano Lett 5:1231. doi:10.1021/nl050788p
28. Guo M, Diao P, Cai S (2005) J Solid State Chem 178:1864. doi:10.1016/j.jssc.2005.03.031
29. Ma T, Guo M, Zhang M, Zhang Y, Wang X (2007) Nanotechnology 18:035605. doi:10.1088/0957-4484/18/3/035605
30. Okada T, Agung BH, Nakata Y (2004) Appl Phys A 79:1417
31. Hartanto AB, Ning X, Nakata Y, Okada T (2004) Appl Phys A 78:299. doi:10.1007/s00339-003-2286-2
32. Kawakami M, Hartanto AB, Nakata Y, Okada T (2003) Jpn J Appl Phys Part 2 Lett 42:L33
33. Konenkamp R, Word RC, Schlegel C (2004) Appl Phys Lett 85:6004. doi:10.1063/1.1836873
34. Fan Z, Dutta D, Chien C-J, Chen H-Y, Brown EC, Chang P-C et al (2006) Appl Phys Lett 89:213110. doi:10.1063/1.2387868
35. Wang ZL, Song J (2006) Science 312:243
36. Wang L, Zhang X, Zhao S, Zhou G, Zhou Y, Qi J (2005) Appl Phys Lett 86:024108. doi:10.1063/1.1851607
37. Wu J-J, Liu S-C (2002) Adv Math 14:215. doi:10.1002/1521-4095(20020205)14:3<215::AID-ADMA215>3.0.CO;2-J
38. Zhang G, Nakamura A, Aoki T, Temmyo J, Matsui Y (2006) Appl Phys Lett 89:113112. doi:10.1063/1.2207832
39. Yi G-C, Park WI, Kim DH, Jung SW (2002) Appl Phys Lett 80:4232. doi:10.1063/1.1434313
40. Park JY, Yun YS, Hong YS, Oh H, Kim J-J, Kim SS (2005) Appl Phys Lett 87:23108
41. Lowndes DH, Geohegan DB, Puretzky AA, Norton DP, Rouleau CM (1996) Science 273:898. doi:10.1126/science.273.5277.898
42. Vanheusden K, Warren WL, Seager CH, Tallant DR, Voigt JA, Gnade BE (1996) J Appl Phys 79:7983. doi:10.1063/1.362349
43. Heo YW, Norton DP, Pearton SJ (2005) J Appl Phys 98:073502. doi:10.1063/1.2064308
44. Liu ZW, Ong CK, Yu T, Shen ZX (2006) Appl Phys Lett 88:053110. doi:10.1063/1.2168675

45. Heo YW, Tien LC, Norton DP, Kang BS, Ren F, Gila BP et al (2004) Appl Phys Lett 85:2002. doi:10.1063/1.1792373
46. Costa PMFJ, Golberg D, Shen G, Mitome M, Bando Y (2008) J Mater Sci 43:1460. doi:10.1007/s10853-007-2307-1
47. Chander R, Raychaudhuri AK (2006) J Mater Sci 41:3623. doi:10.1007/s10853-006-6218-3
48. Liu ZW, Yeo SW, Ong CK (2007) J Mater Sci 42:6489. doi:10.1007/s10853-007-1557-2
49. Heo YW, Kaufman M, Pruessner K, Siebein KN, Norton DP, Ren F (2005) Appl Phys A 80:263. doi:10.1007/s00339-004-2667-1
50. Heo YW, Abernathy C, Pruessner K, Sigmund W, Norton DP, Overberg M et al (2004) J Appl Phys 96:3424. doi:10.1063/1.1774257
51. Yang Z, Huang Y, Chen ST, Zhao YQ, Li HL, Hu ZA (2005) J Mater Sci 40:1121. doi:10.1007/s10853-005-6927-z